LIMNOLOGY and OCEANOGRAPHY

ASLO

Limnol. Oceanogr. 67, 2022, 187–202

doi: 10.1002/lno.11985

Scallop shells as geochemical archives of phytoplankton-related ecological processes in a temperate coastal ecosystem

Julien Thébault,[1*] **Aurélie Jolivet**,[1,2] **Matthieu Waeles**,[1] **Hélène Tabouret**,[3] **Sophie Sabarot**,[1,3] **Christophe Pécheyran**,[3] **Aude Leynaert**,[1] **Klaus Peter Jochum**,[4] **Bernd R. Schöne**,[5] **Lukas Fröhlich**,[5] **Valentin Siebert**,[1] **Erwan Amice**,[1] **Laurent Chauvaud**[1]

[1]Univ Brest, CNRS, IRD, Ifremer, LEMAR, Plouzané, France
[2]TBM Environnement, Auray, France
[3]Universite de Pau et des Pays de l'Adour, UPPA-CNRS, IPREM, Pau, France
[4]Max Planck Institute for Chemistry, Climate Geochemistry Department, Mainz, Germany
[5]Institute of Geosciences, University of Mainz, Mainz, Germany

Abstract

Phytoplankton dynamics in coastal ecosystems is increasingly altered by land-based human activities. Yet, this global vision conceals major disparities, among sites and through time. As conventional monitoring time series are quite sparse and relatively short, biological records of environmental variability appear as relevant tools to gain insights into phytoplankton dynamics over larger temporal and spatial scales. Here, we present results of an interdisciplinary project dealing with chemical information archived in shells of *Pecten maximus* (Bivalvia; Pectinidae), known to form daily growth striae on its shell surface. Several individuals were collected in the Bay of Brest (France) in 2011 and 2012, and analyzed for the molybdenum and lithium concentrations in their soft tissues and the element-to-calcium ratios (Mo : Ca and Li : Ca) in their calcitic striae. All shells revealed high synchrony and reproducibility in their Mo : Ca and Li : Ca profiles, characterized with a major peak at the end of May and in mid-June 2011, respectively. Detailed analysis of physical, chemical, and biological variables measured in seawater during an extensive 9-month environmental survey enabled a meticulous description of phytoplankton dynamics in 2011 and its impact on shell geochemistry. Main findings strongly suggest that (1) the timing of Mo : Ca peaks reflects the occurrence of silicon limitation and diatom aggregation periods, (2) the height of these peaks relates to the amplitude of the first spring diatom bloom, and (3) Li : Ca serves as a proxy for the temporal dynamics of diatom biovolume and of biogenic silica recycling at the sediment–water interface.

Phytoplankton is the cornerstone of the oceans, forming the pedestal of almost all marine food webs. Although making up only 0.2% of the total photosynthetic biomass on Earth, these tiny organisms are responsible for approx. 46% of the annual global net primary production (Field et al. 1998). Among phytoplankton, diatoms are by far the main contributors to global net primary production (approx. 50%), together with coccolithophores and chlorophytes (approx. 20% each), and finally cyanobacteria (approx. 10%; Rousseaux and Gregg 2014). Up to 25% of this production occurs on continental margins (Boyce et al. 2010) that yet occupy a mere 7% of the ocean surface. These shallow-water ecosystems are strongly affected by land-based human activities. For instance, enhanced nitrogen and phosphorus loadings can change the natural ratios between nutrients, leading to quantitative and qualitative alterations in phytoplankton communities. A decrease in the Si/N ratio (due to enhanced nitrogen supply) can result in shifts in phytoplankton communities initially dominated by silicified species (diatoms) toward nonsilicified species (e.g., dinoflagellates) that are sometimes toxic (Cloern 2001).

Given its crucial role in the functioning of oceanic and coastal ecosystems, and more broadly in the global biogeochemical carbon cycle and regulation of the climate of the Earth, it is paramount to characterize the spatial and temporal variabilities of phytoplankton dynamics. This is commonly achieved using remote sensing since the first satellite sensors

*Correspondence: julien.thebault@univ-brest.fr

Additional Supporting Information may be found in the online version of this article.

were launched in the late 1970s. This approach is undoubtedly very useful, specifically because it provides the largest possible spatial coverage. However, its limited temporal extent (approx. two decades) renders the identification of long-term, pluridecadal, trends very difficult. Remote sensing also has significant limitations in coastal waters where high levels of suspended particulate matter and colored dissolved organic matter can significantly influence optical properties of surface waters, thus altering phytoplankton estimates (Blondeau-Patissier et al. 2014).

Conventional monitoring time series (electronic instruments, periodic water sampling) provide reliable information in coastal ecosystems, and are essential to detect, measure, and understand changes in the Earth system and its biological communities. Remarkable long-term, still ongoing, examples are the Helgoland series which started in the German Bight in 1962 (Hickel 1998), and the Continuous Plankton Recorder survey launched in the North Sea and North-East Atlantic in 1948 (Warner and Hays 1994). However, most other observational phytoplankton records are too short to encompass natural low-frequency cycles in coastal environments. Moreover, such data sets are relatively scattered and thus poorly replicated. Some studies attempted to combine transparency-derived (Secchi disk measurements) and in situ chlorophyll data in order to get longer records (110 years long; Boyce et al. 2010) but such data blending could lead to significant biases in the estimation of chlorophyll *a* (Chl *a*) concentration (Mackas 2011). Therefore, the development of new tools aiming at reconstructing long-term, high-resolution, estimates of phytoplankton dynamics are necessary to get a better understanding of macroecological changes in coastal ecosystems.

Within this framework, biogenic archives of environmental variability may embody a valuable approach for extending phytoplankton records over longer time scales. Indeed, corals, sclerosponges, coralline algae, or mollusk shells form their external calcium carbonate skeleton periodically, leading to the accretion of growth increments and lines (aka "striae" in pectinids). Providing their periodicity of formation is known, these structures can in turn serve as chronological benchmarks to place each portion of a given archive into precise temporal context (a major component of the research field of "sclerochronology"). Corals, sclerosponges and coralline algae are powerful tools for investigations on past environmental variability with a seasonal to annual resolution. However, in highly dynamic systems such as coastal waters, many ecological processes such as phytoplankton blooms occur on daily or weekly time scales. From that prospect, bivalve mollusk shells appear as outstanding archives for high-resolution paleoecological studies because many species form distinct daily growth patterns. These biocarbonates can therefore provide detailed, daily-resolved records of environmental variables. The latter are archived in shells in the form of geochemical properties such as stable isotopes and minor and trace elements (Peharda et al. 2021).

Most studies dealing with geochemical composition of bivalve shells focused on proxies for seawater temperature. Yet, their potential as archives for phytoplankton dynamics has been overlooked. Historically, such studies first attempted to use the stable carbon isotope composition of shells as a paleoproductivity proxy, reflecting the isotope signature of dissolved inorganic carbon (Mook and Vogel 1968). However, the $\delta^{13}C_{shell}$ values often also reflect the isotope signal of metabolic carbon that ends up in the shell during shell formation (Marchais et al., 2015). Inspired by deep-sea oceanographic studies, the barium-to-calcium ratio (Ba : Ca) measured in shells has long been the most promising tool to assess phytoplankton dynamics. Indeed, ontogenetic variations of Ba : Ca have a similar profile in many bivalve species, that is, a background value (with variations possibly reflecting changes in salinity; Poulain et al. 2015) interrupted by sharp peaks which are often synchronous between contemporaneous specimens from the same locality (Doré et al. 2020). Phytoplankton blooms (especially diatoms) have often been put forward as the most likely drivers of Ba : Ca peaks in shells. However, this relationship is definitely not straightforward, and factors controlling Ba : Ca variations are still puzzling and not sufficiently understood (Gillikin et al. 2008).

More recently, molybdenum-to-calcium (Mo : Ca) and lithium-to-calcium (Li : Ca) ratios in bivalve shells have been suggested as promising proxies for phytoplankton bloom dynamics (Thébault et al. 2009*a*; Barats et al. 2010; Thébault and Chauvaud 2013; Sadatzki et al. 2019). However, the influence of phytoplankton dynamics on Mo and Li incorporation in bivalve shells has been put in doubt in two recent studies on common cockles and Arctic bivalves (Füllenbach et al. 2015; Vihtakari et al. 2017). Undoubtedly, the extreme scarcity of studies dealing with Mo and Li prevents conclusions about the exact mechanisms behind their incorporation into bivalve shells. More studies are required to determine how faithful Mo : Ca and Li : Ca ratios archived in shells record changes in phytoplankton biomass and composition in coastal ecosystems.

In summary, existing proxies for phytoplankton dynamics in bivalve shells are still not well constrained. The present study thus focuses on Mo : Ca and Li : Ca ratios in shells of *P. maximus* from the Bay of Brest (France). This scallop species has major advantages for sclerochronological investigations, including a rapid shell growth rate (up to several hundreds of micrometers per day) and the presence of clearly visible annual and daily external growth lines on its shell (Fig. 1). This common species has a biogeographical distribution spanning the entire European Atlantic coastline, extending from Northern Norway (Lofoten islands) to Southern Portugal (and beyond to Morocco via Azores). Moreover, it has many very close relative species all over the world, with very similar characteristics (e.g., *Pecten jacobeus* in the Mediterranean, *Pecten fumatus* in Australia, *Pecten albicans* along the coasts of Japan and China, *Pecten novaezelandiae* endemic to New Zealand,

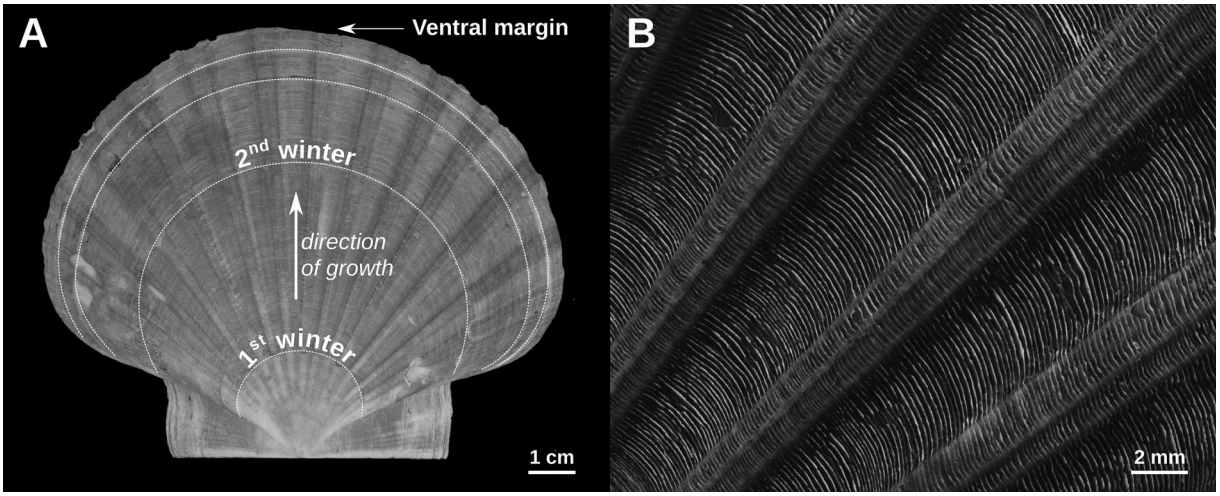

Fig. 1. (**A**) Outer shell surface of the left valve of *Pecten maximus* from the Bay of Brest. Dashed lines = annual (winter) growth checks. (**B**) Magnified portion showing daily growth striae.

Pecten sulcicostatus in South Africa, or *Leopecten diegensis* from California and Mexico). Any calibration of proxies for phytoplankton dynamics on *P. maximus* might be applied to these other scallop species, thus opening up new, amazing horizons.

The primary goal of this paper is to get a better understanding of ecological processes driving the incorporation of Mo and Li into *P. maximus* shells from the Bay of Brest. To this end, we retrieved ontogenetic, sub-weekly resolved, time series of Mo : Ca and Li : Ca in shells of 16 contemporaneous specimens which differed in their ontogenetic age and sampling locality. This unique data set was then compared with numerous environmental data obtained from a high-frequency monitoring station located next to the scallop population. Our ultimate objective was to develop new, high-resolution, temporally well-constrained, and robust proxies for phytoplankton dynamics in coastal ecosystems.

Material and methods

Study area

Our study site, the Pointe de Lanvéoc (48°17′39″N–4°27′12″W), is located in the southern part of the Bay of Brest (Brittany, Northwest France; Fig. 2). The Bay of Brest is a semi-enclosed, macro-tidal, marine ecosystem of 180 km^2 connected to shelf waters (Iroise Sea, North-East Atlantic) by a narrow and deep strait (2 km width, 40 m max. depth). The bay itself is a shallow basin with an average depth of 10 m. The shoals are relatively wide, and only 15% of the total area is deeper than 20 m. Two rivers, the Aulne (catchment area = 1792 km^2) and the Elorn (catchment area = 379 km^2), are responsible for up to 80% of the total freshwater input into the bay. The fieldwork was carried out between gabions #2 and #3 of the former oil terminal jetty, approx. 150 m north of the shore (average depth at mid-tide = 10 m). The floor is characterized by mixed sandy and silty sediments, with significant amounts of large biogenic detritus (shells, calcareous algae).

Environmental monitoring

An environmental survey was carried out between 01 February 2011 and 24 October 2011 (52 cruises on the R/V Albert-Lucas). Between March and May (i.e., spring bloom period), the sampling frequency was twice per week, and approx. once per week during the remaining time. To facilitate comparisons between the cruises, water samples were collected around mid-tide, using 5- and 12-L Niskin sampling bottles. Samples were retrieved from subsurface (−1.5 m), mid-depth (−5 m), and bottom water (−8 to −13 m) (mean = −10.2 m, depending on the tide level). They were subsequently analyzed for the concentration in Chl *a* and phytoplankton species (only in bottom water samples), particulate organic carbon (POC), nitrates (NO_3^-), dissolved silicate, dissolved molybdenum (DMo), and particulate molybdenum (PMo). Seawater salinity and temperature were obtained from a conductivity-temperature-depth (CTD) profiler (SeaBird SBE19). Description of the methods used to analyze these environmental parameters is presented as Supporting Information (Methods SM1). The Aulne River water discharge data were retrieved from the Agence de l'Eau Loire-Bretagne (Châteaulin gauging station).

Shell sampling

Live scallops were collected using SCUBA diving at each cruise. All of them were individuals of age class II (i.e., specimens that have lived through two 1st of January, therefore showing two annual (winter) growth lines on their left [flat] valve) in order to get a sufficient mass of soft tissues for elemental analyses (and also because age class I specimens were too small to be pinpointed by SCUBA divers in the first

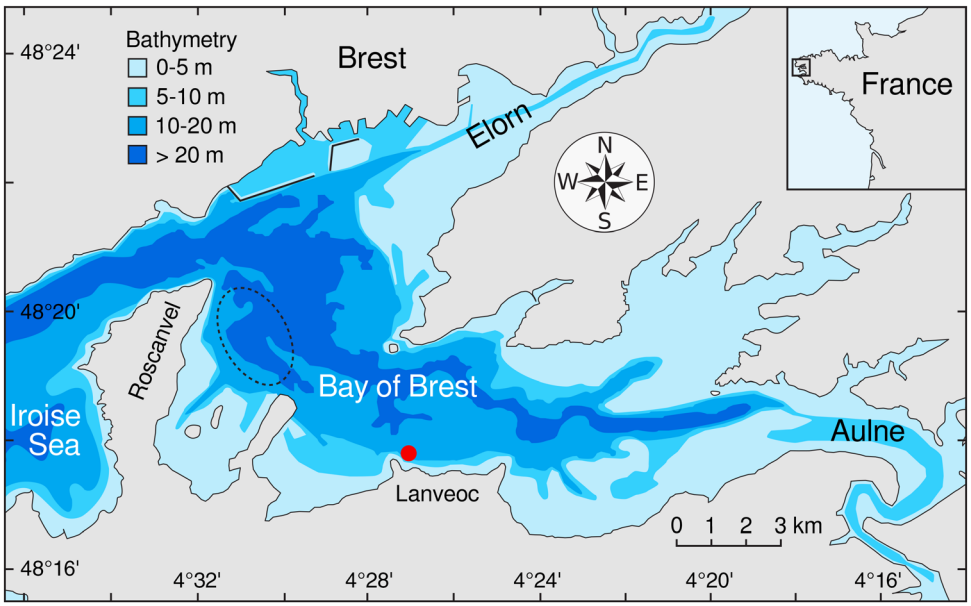

Fig. 2. Shell sampling locality in the Bay of Brest, North-West France (Pointe de Lanvéoc: filled red circle; Roscanvel bank: dashed ellipse).

half of the environmental survey). These specimens were sacrificed immediately after return to the laboratory (within 3 h after collection). The mantle, gills, gonad, digestive gland, and adductor muscle were dissected from each specimen (in this order). Dissecting tools were cleaned with 95% ethanol after removal of each organ. All soft tissues were weighed to the nearest mg, frozen at −20°C and then freeze-dried. These samples were finally chemically characterized (lithium and molybdenum).

By the end of the survey, age class I scallops were large enough to be observed by divers and nine of them were harvested on 30 August 2011 (three shells) and 24 October 2011 (six shells). The left valves of these specimens were then analyzed for their Li and Mo content incorporated during the 1st full year of growth, that is, between the 1st winter growth check and the ventral margin (Fig. 1). Four age class II specimens were also collected in October 2011 to identify potential age-related differences in Li and Mo profiles of the shells. For these four specimens, chemical analyses were performed on the shell portion between the 2nd winter growth check (line) and the ventral margin.

In order to check whether the element content in shells from Lanvéoc reflects the skeletal concentrations in other scallops from the Bay of Brest, three age class II specimens were collected alive by dredging on Roscanvel bank (water depth = approx. 25 m; distance from Lanvéoc = approx. 6 km; Fig. 2) on 05 January 2012. Their left valves were also studied for Li and Mo incorporated during calendar year 2011, that is, when these individuals were still age class I scallops. Detailed information on the 16 scallops used for shell geochemical analyses are presented in Supporting Information Table S1.

Growth and elemental analyses in scallop shells

Prior to shell growth and chemical analyses, left valves of all specimens listed in Supporting Information Table S1 were cleaned by soaking in 90% acetic acid for 30–45 s, rinsed with deionized water and air-dried. Daily shell growth rates were determined by measuring distances between successive striae along the axis of maximum growth using image analysis software (ImageJ). Based on the daily periodicity of stria formation, each shell portion was placed in precise temporal context by backdating from the last stria deposited at the day of collection.

Trace element content in these shells was analyzed using two different techniques, in three different laboratories (Supporting Information Table S1). Shells A–C were investigated at Pôle Spectrométrie Océan (PSO, France) using solution nebulization inductively coupled plasma mass spectrometry. Shells D–S were measured using a laser ablation unit coupled with an inductively coupled plasma mass spectrometer, either at the Max Planck Institute for Chemistry (MPIC, Germany) or at the Institute of Analytical Sciences and Physico-Chemistry for Environment and Materials (IPREM, France). Detailed description of the methods used in these laboratories is presented as Supporting Information (Methods SM2). Whatever the methodology used for trace element analyses in shells, the sampling strategy consisted in recovering 1.8–2.7 samples per week of growth (except for analyses performed at MPIC where the resolution was set to 6.6–6.8 samples per week). All results are expressed as molar ratios to calcium (in μmol mol^{-1}).

Differences in molar ratios between study sites (Lanvéoc vs. Roscanvel, for age class I scallops analyzed at IPREM), and between ontogenetic age (age class I vs. age class II, for

scallops collected at Lanvéoc and analyzed at IPREM) were assessed with Wilcoxon tests. Statistical analyses were performed on R version 3.6.3 (R Core Team 2020).

Elemental analyses in soft tissues

Freeze-dried soft tissues of 30 age class II scallops collected between 28 April 2011 and 27 June 2011 (i.e., the time interval during which the shell Li and Mo content showed the largest variations) were finely ground in an agate mortar, carefully cleaned with 95% ethanol between each sample. Digestion was carried out with 100 mg of ground tissue, except for the adductor muscle (400 mg as this tissue had the lowest Li and Mo concentrations) and the certified reference materials (200 mg). The latter were lobster hepatopancreas (NRCC TORT-3), fish proteins (NRCC DORM-4), and dogfish liver (NRCC DOLT-5). Description of the method used to analyze these samples is presented in Supporting Information (Methods SM3).

Results

Element-to-calcium ratios in scallop shells

Irrespective of the analytical method, study site or age class, all shells revealed similar Mo : Ca (Fig. 3A) and Li : Ca profiles (Fig. 3B). They were characterized by a relatively flat background around 0.05 and 40 μmol mol^{-1} for Mo : Ca and Li : Ca, respectively. A large Mo : Ca peak occurred in all specimens at the end of May 2011 (maximum value reached between 22 May 2011 and 01 June 2011), ranging from 0.179 μmol mol^{-1} (shell D, on 27 May 2011) to 0.474 μmol mol^{-1} (shell H, on 25 May 2011). Similarly, a large Li : Ca peak was measured in all shells in mid-June 2011: The maximum value (116 μmol mol^{-1} in shell B, 392 μmol mol^{-1} in shell N) was reached between 14 and 20 June 2011.

Shells sampled at Roscanvel (specimens K, L, and M) had Mo : Ca ($W = 4758$, $p < 0.001$) and Li : Ca ($W = 4005$, $p < 0.001$) median values significantly higher than shells collected at Lanvéoc and measured in the same laboratory (specimens G, H, and J). However, Mo : Ca peaks were of similar height (0.257 μmol mol^{-1} at Roscanvel vs. 0.286 μmol mol^{-1} at Lanvéoc), as were Li : Ca peaks (203 and 161 μmol mol^{-1} at Roscanvel and Lanvéoc, respectively).

Furthermore, the comparison between Lanvéoc shells analyzed at IPREM for their 1st and 2nd year of growth did not reveal significant differences for Mo : Ca ratios ($W = 3019$, $p < 0.001$). On the other hand, Li : Ca had a higher median value and presented a more intense peak in shell portions formed after the 2nd winter growth check in comparison with shells during their 1st full year of growth ($W = 3742$, $p = 0.052$).

Although significant differences were highlighted in the distribution of trace element data in shells sampled at different study sites, and came from specimens of different ontogenetic age, Mo : Ca and Li : Ca time series of the different specimens were very similar. More specifically, the timing and order of magnitude of Mo : Ca peaks were very close in all 16 specimens. The same also applied for Li : Ca profiles. For these reasons, average Mo : Ca and Li : Ca time series were calculated based on the nine shells collected at Lanvéoc and analyzed for the 1st full year of growth (i.e., specimens A–J; Fig. 4).

The relatively low inter-individual variability of Mo : Ca and Li : Ca profiles and the strong synchronicity of their main peak clearly appears in Fig. 4. The maximum Mo : Ca values occurred on 27 May 2011 ($\pm$ 2 d) and reached, on average, 0.233 $\pm$ 0.039 μmol mol^{-1} (mean $\pm$ 95% confidence interval; Fig. 4A). Several small increases were observed during summer 2011; however, their intensity was always lower than 0.082 μmol mol^{-1}. The average Li : Ca profile also showed one main peak (159 $\pm$ 37 μmol mol^{-1}; Fig. 4B), which occurred 3 weeks after the Mo : Ca peak (maximum value at 18 June 2011 $\pm$ 2 d). No other significant Li : Ca peak was observed before or after mid-June.

Molybdenum and lithium concentrations in soft tissues

The Mo concentration progressively increased in all soft tissues between the end of April and the end of May 2011 (Fig. 5A). However, this increase was more important in the digestive gland (approx. sixfold increase from 9.8 to 55.9 μg g^{-1}) than in the other tissues (twofold to threefold increase with maximum concentration < 10 μg g^{-1}). This concentration suddenly dropped in early June before reaching a second, less intense, peak on 20 June 2011. The latter was likewise stronger developed in the digestive gland than in the other soft parts. As for lithium, its concentration gradually increased from 0.3–0.6 μg g^{-1} in late April to 2.2–4.7 μg g^{-1} on 20 June 2011 (Fig. 5B). The increase was almost identical in all organs. The most remarkable boost was measured in the gills and the mantle (10- and 9-fold increase, respectively) while the Li concentration only increased fourfold in the digestive gland. At the end of June 2011, the highest concentrations were detected in the mantle, the gills, and the gonad, respectively. It is noteworthy that Mo and Li concentration maxima in soft tissues occurred at the same time ($\pm$ 2 d) as the maximum respective ratios in the shell calcite.

Daily shell growth rates

Average daily shell growth rate after the 1st winter growth check ranged from approx. 50 μm d^{-1} in late February 2011 to maximum values around 280 μm d^{-1} in summer (Supporting Information Fig. S1). Shell growth dynamics presented a rapid increase from approx. 60 μm d^{-1} in mid-March to approx. 250 μm d^{-1} 5 weeks later. A sudden growth rate reduction was observed in early May 2011, with values decreasing from 250 to 180 μm d^{-1} in 5 d (−28%). This event occurred simultaneously with the main spring phytoplankton bloom. Daily shell growth rate stayed around 250 μm d^{-1} from early June to mid-July and then started to decrease gradually until the end of the growing season in fall of 2011.

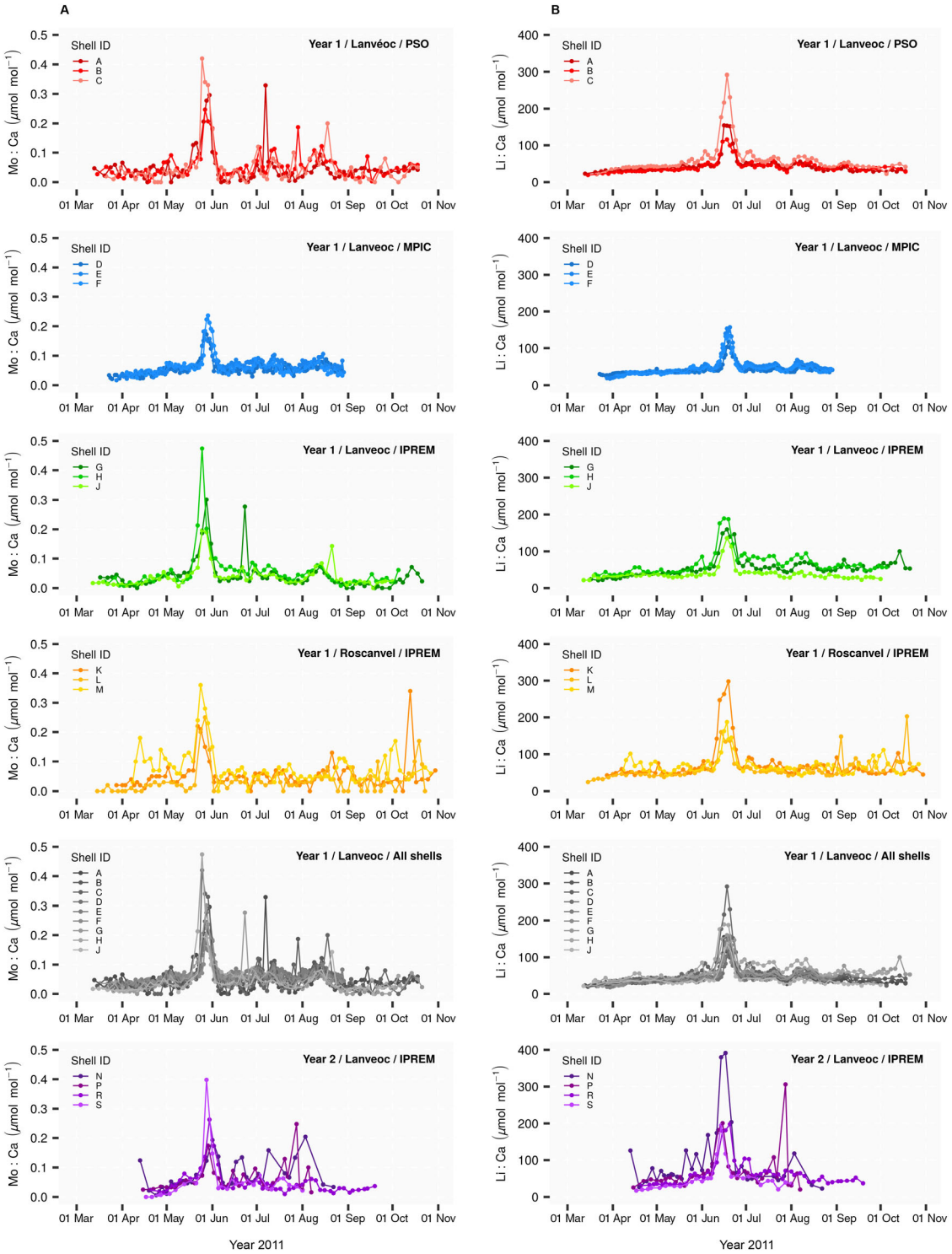

Fig. 3. Element-to-calcium ratio time series in the 16 scallop shells, grouped according to their age class, sampling locality and laboratory/method where analyses were carried out. (**A**) Mo : Ca. (**B**) Li : Ca.

Phytoplankton dynamics

As the water column was well mixed throughout the environmental survey, no significant differences were observed in physical, chemical, and biological parameters at the three different depths. Stratification was never observed on this site. Therefore, only average values will be presented, representing

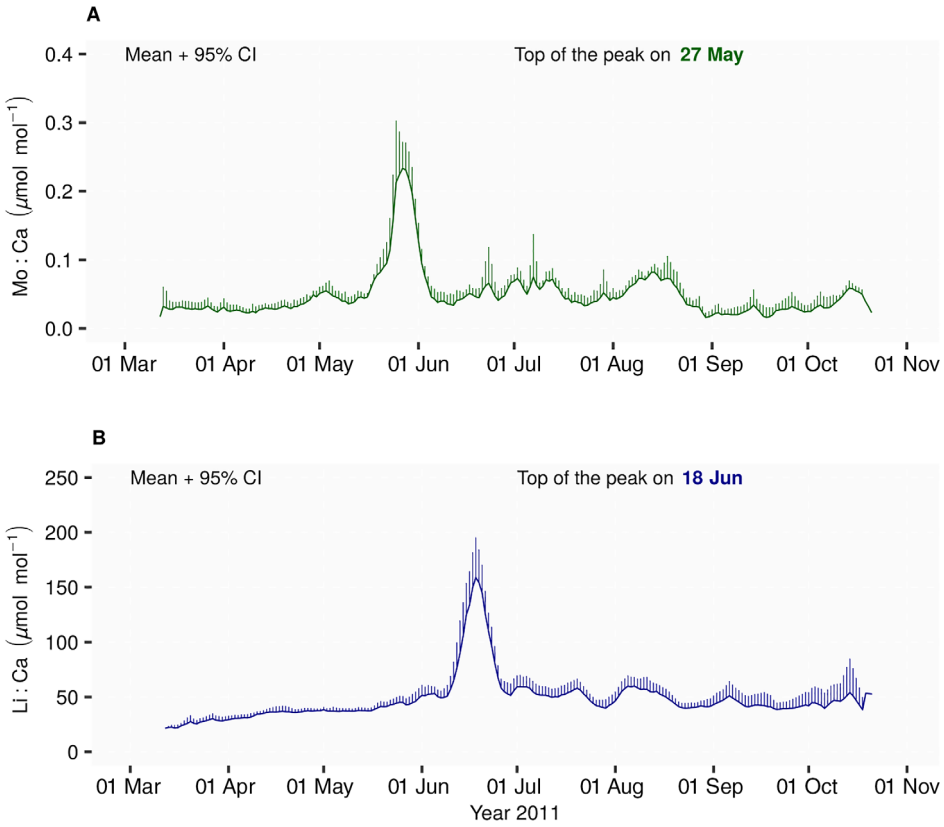

Fig. 4. Average time series of Mo : Ca (**A**) and Li : Ca (**B**) ratios determined between the 1st winter growth check and the ventral margin of nine scallop shells collected at Lanvéoc (mean + 95% upper confidence interval).

environmental conditions in the entire water column, except for phytoplankton taxonomy, which was only investigated in bottom-water samples.

Chl *a* concentration gradually increased from 0.62 $\mu g\,L^{-1}$ on 08 February 2011 to 5.05 $\mu g\,L^{-1}$ on 05 May 2011, when the annual maximum concentration was reached (Fig. 6A). A secondary spring bloom was observed on 06 June 2011, reaching 3.34 $\mu g\,L^{-1}$. While Chl *a* concentration was quite low during summer, two other blooms were detected in late summer and early fall (30 August 2011: 2.77 $\mu g\,L^{-1}$; 03 October 2011: 3.54 $\mu g\,L^{-1}$). Following size-fraction analyses, the temporal variations of chloropigment concentration were mostly explained by large cell dynamics (> 10 μm) all along the survey.

Taxonomic identification of phytoplankton species revealed that diatoms represented 35.8% of all cells sampled at Lanvéoc, while other species belonged to dinoflagellates (7.7%) and nanoflagellates (56.5%). Among diatoms, the most abundant taxa (> 1% of total phytoplankton cell counts) were *Chaetoceros* spp. (81.7% of all diatoms/29.3% of all phytoplankton species), *Dactyliosolen fragilissimus* (5.3%/1.9%), *Guinardia delicatula* (3.7%/1.3%), and *Leptocylindrus danicus* (3.1%/1.1%). Only two dinoflagellates taxa accounted for more than 1% of total phytoplankton cells: *Gymnodinium* spp. (53.4% of all dinoflagellates/4.1% of all phytoplankton species) and *Heterocapsa minima* (40.2%/3.1%). While the main diatom bloom reached a cell concentration of 4.07×10^6 cells L^{-1} (on 06 June 2011), the highest dinoflagellate count was measured on 23 May 2011 with only 0.35×10^6 cells L^{-1}.

All four main Chl *a* concentration increases occurred as a result of diatom blooms (Fig. 6B). More precisely, the two main spring blooms were mostly composed of *Chaetoceros* spp., which represented 49% of the 0.70×10^6 cells L^{-1} on 05 May 2011 (together with 27% *Cerataulina pelagica* and 11% *D. fragilissimus*), and 99% of the 4.11×10^6 cells L^{-1} on 06 June 2011. The relatively high Chl *a* concentration in late summer/early fall (from 30 August 2011 to 03 October 2011; 1.4–3.5 $\mu g\,L^{-1}$) was mostly explained by the abundance of nanoflagellates (35.1–92.2% of total phytoplankton over this period), topped with blooms of *G. delicatula* on 30 August 2011 (19.2% of total phytoplankton) and 03 October 2011 (18.6%).

Interestingly, the main Mo : Ca peak in scallop shells (and highest Mo concentration in soft tissues) occurred 3 weeks after the largest phytoplankton bloom of 2011. Another noteworthy feature was the maximum Li concentration in shells and tissues, which arose approx. 2 weeks after the largest diatom (*Chaetoceros* spp.) bloom of the year.

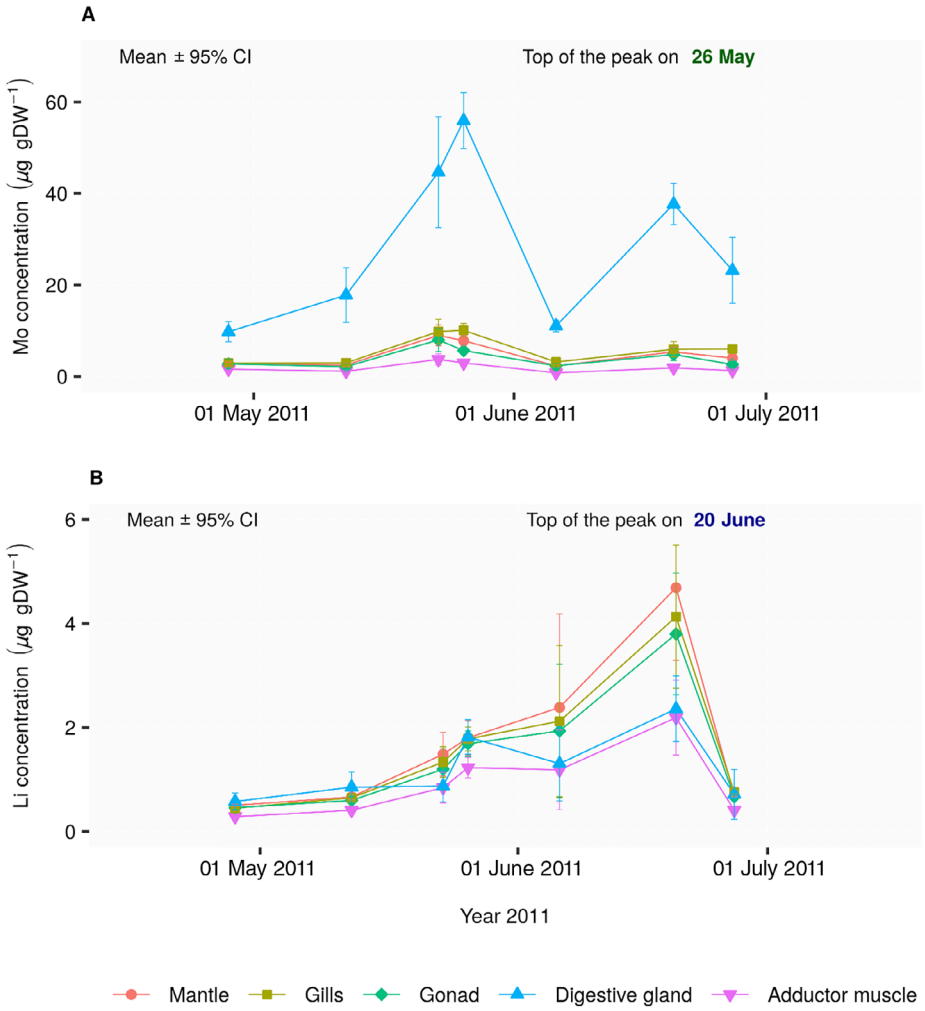

Fig. 5. Time series of trace element concentrations in *Pecten maximus* soft tissues during the spring bloom (**A**: molybdenum; **B**: lithium). Each point represents the average of three to six specimens (except on 27 June 2011 when only two scallops were dissected).

Physicochemical properties of the water column

Water temperature steadily increased from 8.7°C in early February to 16.1°C in late June 2011 (Supporting Information Fig. S2). Over the same period, salinity ranged from 33.0 to 35.1 and covaried inversely with the Aulne River water discharge, which decreased from approx. 55 $m^3\ s^{-1}$ at the end of February to < 2 $m^3\ s^{-1}$ at the end of June 2011 (Supporting Information Fig. S2).

Nitrate and silicate concentrations reached their annual maxima in late winter (Fig. 7). Nutrient stocks rapidly decreased between early March and late April 2011, synchronously with a drop in freshwater discharge and with the onset of phytoplankton growth. Silicates were exhausted on 05 May 2011 (0.03 μmol L^{-1}), exactly at the same time when total Chl *a* concentration reached its annual maximum. Their concentration gradually increased after this date until the end of the environmental survey in late October 2011. While there were still some nitrates in the water column when silicates were exhausted in spring (0.5 μmol L^{-1}), their stock was considered as totally depleted a few days later (0.08 μmol L^{-1} on 09 May 2011). It remained very low (< 0.5 μmol L^{-1}) all summer long, and started to replenish slightly in September and October 2011.

PMo concentrations increased from values under 0.1 nmol L^{-1} in early April to approx. 0.5 nmol L^{-1} in early May 2011 (Fig. 8A). By contrast to Chl *a* concentration which dropped after 05 May 2011 (Fig. 7), PMo concentration continued to increase until 23 May 2011 when it reached its spring maximum (1.2 nmol L^{-1}), and finally dropped in late May back to its winter concentration. DMo concentration, on the other hand, only showed small variations between February and June 2011, ranging from 63.3 nmol L^{-1} on 07 April 2011 to 99.4 nmol L^{-1} on 06 June 2011.

POC concentration, which was in the range 7–22 μmol L^{-1} until mid-April, started to increase in the third week of April with the onset of phytoplankton growth and reached a

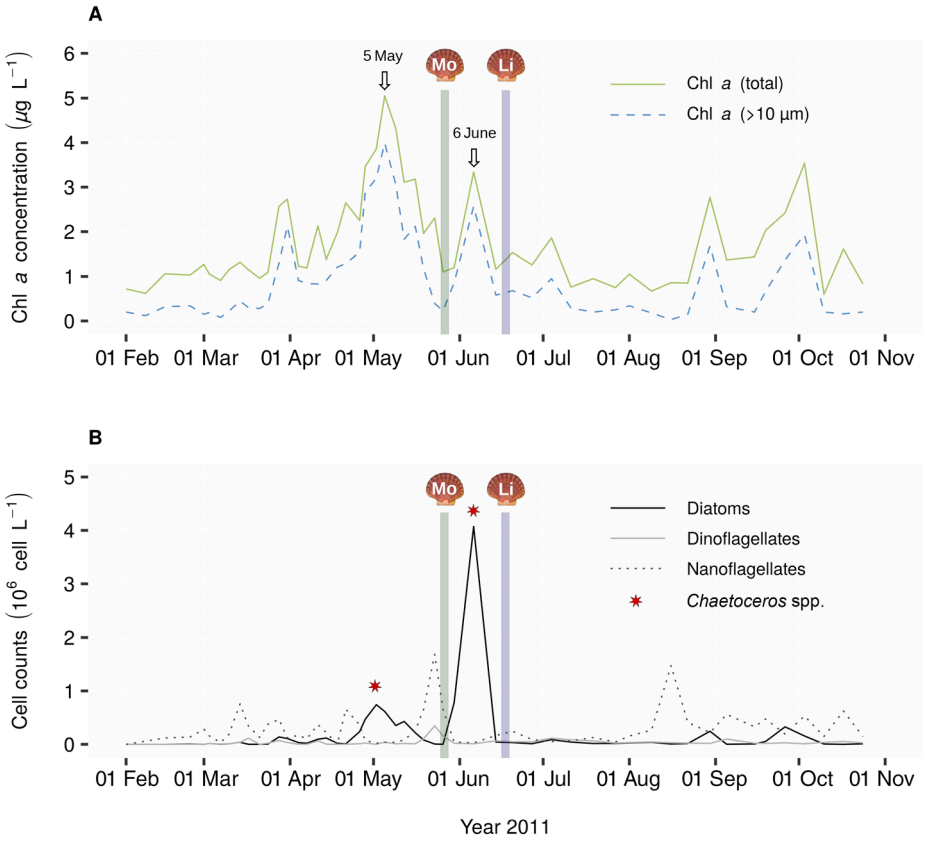

Fig. 6. Phytoplankton dynamics between February and October 2011. (**A**) Time series of chlorophyll *a* concentration (solid line: total concentration; dashed line: size fraction > 10 μm). (**B**) Temporal variations of the composition of phytoplankton communities (black solid line: diatoms; gray solid line: dinoflagellates; dotted black line: nanoflagellates). Red stars indicate the timing of the two largest *Chaetoceros* spp. blooms. Vertical lines show the dates when Mo : Ca and Li : Ca peaks were observed in scallop shells.

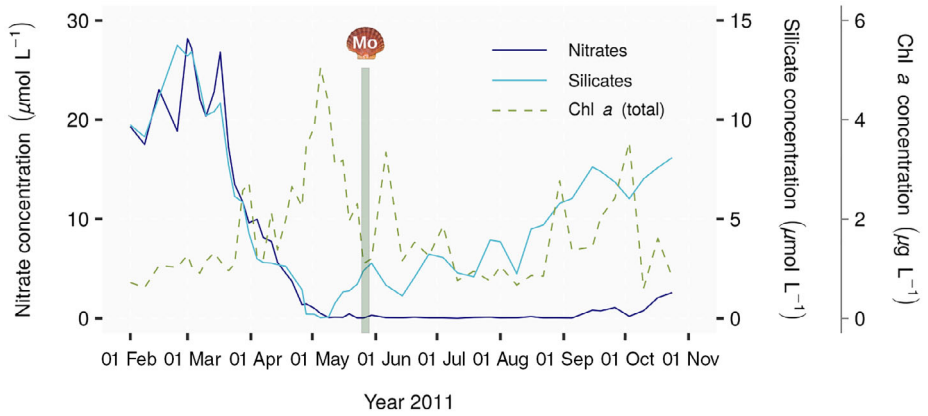

Fig. 7. Time series of nutrient and chlorophyll *a* concentrations between February and October 2011. Vertical line indicates the date of the main Mo : Ca peak in shells.

maximum value of 41 μmol L^{-1} on 09 May 2011 (Fig. 8B). According to the phytoplankton survey, this POC increase corresponded mainly to a diatom bloom (*Chaetoceros* spp.; Fig. 6). The PMo/POC molar ratio in these particles revealed a first increase between late March (2.8 μmol mol^{-1} on 28 March 2011) and mid-May (29.7 μmol mol^{-1} on 16 May 2011), followed by a second, abrupt, rise until the spring maximum was reached on 19 May 2011 (58.8 μmol mol^{-1}). Both PMo

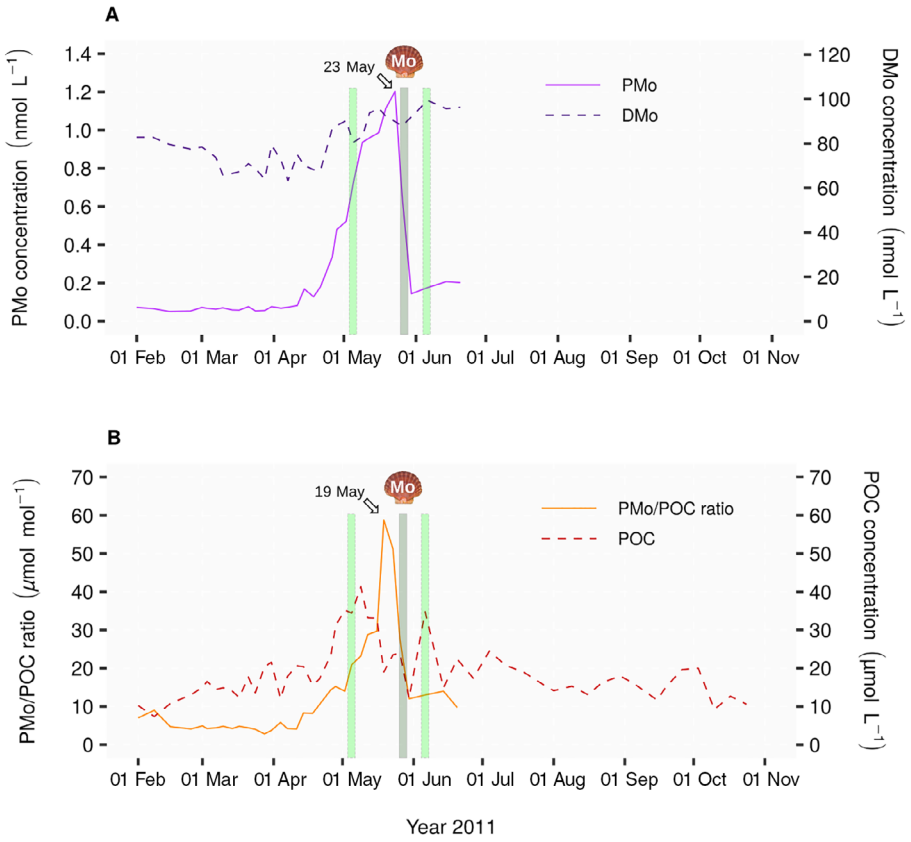

Fig. 8. (**A**) Time series of molybdenum concentration in the water column (dissolved and particulate fractions) between February and June 2011. (**B**) Time series of particulate organic carbon concentration between February and October 2011, and variation of the PMo/POC ratio from February to June 2011. Vertical lines indicate the dates of the main Mo : Ca peak in shells and the two largest spring phytoplankton blooms (*Chaetoceros* spp.).

concentrations and PMo/POC ratio then rapidly dropped close to baseline values within 10 d.

Discussion

Spring bloom dynamics

The 2011 spring phytoplankton dynamics in the Bay of Brest was characterized by a first, plurispecific (*Chaetoceros* spp., *Ce. pelagica*, and *D. fragilissimus*) diatom bloom in early May, followed by a second, monospecific (*Chaetoceros* spp.) diatom bloom in early June (Fig. 6). While the Chl *a* concentration reached its annual maximum during the first bloom, the maximum phytoplankton cell concentration was observed during the second bloom. This can be explained with the different sizes and biovolumes of the diatom species involved in these two blooms. *Chaetoceros* spp. have relatively small cells while *Ce. pelagica* and *D. fragilissimus* are usually large diatoms (with biovolumes approx. one order of magnitude higher than *Chaetoceros* spp.; Olenina et al. 2006). Considering (1) the diatom cell concentrations during the first and second spring blooms, (2) the respective contributions of *Chaetoceros*, *Cerataulina*, and *Dactyliosolen*, and (3) a 1 : 10 ratio for biovolumes of *Chaetoceros* and *Cerataulina*/*Dactyliosolen* single cells, we estimated that the diatom total biovolume could have been only 1.4 times higher during the second bloom. This suggests that the total phytoplanktonic biovolumes (and, therefore, Chl *a* concentrations) were likely comparable between these two spring blooms, despite very different phytoplankton cell quantities.

Such temporal dynamics is not unusual in the Bay of Brest. Quéguiner and Tréguer (1984) observed a late spring bloom in 1981, almost monospecific and dominated by the small colony-forming diatom *Chaetoceros sociale*, which reached very high cell concentrations (up to 12×10^6 cells L^{-1}) with moderate Chl *a* concentration compared with the first spring blooms. Identical conditions were also noticed in 1992 when Ragueneau et al. (1994) observed a large (3×10^6 cells L^{-1}) *Ch. sociale* bloom in mid-June (accounting for 99% of diatoms and 83% of total cell concentration), although Chl *a* concentration was comparatively low (2 μg L^{-1}).

This vigorous spring phytoplankton dynamics can partly be explained by the relatively high nutrient concentrations at the end of winter. The latter gradually decreased from early March onward. This can be explained by several factors including (1) weaker freshwater inputs (Aulne River water discharge decreasing from 45 m^3 s^{-1} in early March to 5 m^3 s^{-1}

in late April; Supporting Information Fig. S2), (2) continuous water tidal exchange with the Iroise Sea, and (3) phytoplankton growth. The comparison between in situ nutrient concentrations to half-saturation constants for nutrient uptake (K_m) is an interesting approach to highlight nutrient limitation. According to Del Amo et al. (1997), K_m values for dissolved inorganic nitrogen and silicates in the Bay of Brest are close to 2 μmol L^{-1}. Nutrient concentrations below this threshold correspond to stressful nutritional conditions limiting phytoplankton growth. Nitrate and silicate concentrations dropped below their K_m values between 21 and 26 April 2011, although the maximum Chl *a* concentration was reached approx. 1.5 weeks later. However, another nitrogen source could have been used for phytoplankton growth, namely dissolved organic nitrogen. The latter has been recognized as an important N source for phytoplankton communities. Urea and free amino acids can substantially contribute to the spring bloom production in coastal waters (Moschonas et al. 2017). Unfortunately, dissolved organic nitrogen concentration was not measured during this survey. Nevertheless, it is admitted that it frequently exceeds that of dissolved inorganic nitrogen in both marine and freshwater ecosystems (Berman and Bronk 2003). Therefore, as already noticed by Del Amo et al. (1997), silicon was likely the primary limiting factor in the Bay of Brest, responsible for the collapse of the first, diatom-dominated, spring bloom.

While silicates were already limiting growth at the end of April, diatom cells kept on photosynthesizing for a few days under nutrient stress. Such conditions are known to accelerate diatom sinking and to result in the formation of aggregates in the water column. Indeed, many diatom genera (including *Chaetoceros*) can form aggregates (marine snow) when their cells collide and then stick together (Alldredge and Gotschalk 1989). Diatom stickiness is strongly affected by the production of extracellular polymeric substances which increases under nutrient limitation (Thornton 2002). Production of such substances can then lead to the formation of transparent exopolymeric particles which are major agents of diatom aggregation (Passow 2000). Crocker and Passow (1995) noticed that *Chaetoceros* can cause aggregation by generating transparent exopolymeric particles which, in turn, scavenge cells into aggregates. Conditions for diatom aggregate formation were certainly met in the Bay of Brest in early May 2011: The development of a large bloom mostly consisted of diatoms (dominated by *Chaetoceros*) and occurred under nutrient limitation.

This hypothesis is reinforced with scallop daily shell growth rate which was strongly reduced in early May 2011 (−28% in 5 d; Supporting Information Fig. S1). Spring shell growth retardations are quite common in *P. maximus* from the Bay of Brest. They have often been explained by the sedimentation of large diatom aggregates (especially *Chaetoceros*) which affects food intake and/or respiratory activity of the scallops by gill clogging or oxygen depletion (Lorrain et al. 2000).

The second spring bloom observed in early June 2011 in the Bay of Brest was almost monospecific (99% *Chaetoceros*). Its development was sustained by relatively high levels of silicates (above K_m values in early June; Fig. 7), probably originating from biogenic silica dissolution on the seafloor. Ragueneau et al. (1994) already pointed out that silicon recycling at the sediment–water interface is the main contributor to the silicate pool responsible for the late spring bloom in the Bay of Brest. Nitrate pool was not replenished in early June (Fig. 7), but the June *Chaetoceros* bloom may have used nitrogen from the dissolved organic nitrogen pool. As the water column was not nutrient-limited in early June, it is unlikely that this bloom formed aggregates. This statement is reinforced by the lack of shell growth retardation in June (Supporting Information Fig. S1).

Locality and age effects on scallop shell chemistry

In order to check whether Mo : Ca and Li : Ca time series differed among collection sites in the Bay of Brest and according to the ontogenetic age of the scallops, we analyzed three batches of shells in the same laboratory to preclude methodology-related discrepancies (IPREM): (1) 1st year of growth in specimens collected at Lanvéoc and Roscanvel, and (2) specimens belonging to different age classes (1st and 2nd year of shell growth) collected at the same locality (Lanvéoc).

Whereas the Mo : Ca and Li : Ca background levels were slightly higher in shells from Roscanvel (difference reflected in a statistically higher median value compared with shells from Lanvéoc), the Mo : Ca and Li : Ca peak heights were very similar at both localities (Fig. 3). However, the most striking feature is the synchronicity of respective peaks in shells from the two sites. The main Mo : Ca peak occurred 1 day earlier in shells from Roscanvel (24 May 2011) compared with those from Lanvéoc. This difference is likely not significant given the sampling strategy set to laser ablation every third stria. As for the spring Li : Ca peak, it appeared on the exact same date (18 June 2011) at both localities.

Such a synchronicity suggests that the environmental phenomenon responsible for the incorporation of large amounts of Mo and Li in scallop shells likely occurred at a large spatial scale. At Roscanvel, scallops were harvested in relatively deep waters (−25 m), closer to the strait connecting the bay to the Atlantic Ocean, in comparison with specimens collected in shallow waters (approx. -10 m) from Lanvéoc. This study site is more subject to the influence of the Aulne estuarine waters than Roscanvel. Despite these major discrepancies, trace element profiles in scallop shells were very similar, suggesting that both habitats experienced a similar springtime event in the well-mixed water column.

Geochemical analyses in *P. maximus* are usually performed on the shell portions formed between the 1st and 2nd winter growth check. The reason behind this strategy is that scallops of this age class have the longest annual growing season and thus accumulate the longest annual geochemical record. In

addition, their daily shell growth rates are higher than on age class II+ scallops, which enable a better temporal resolution in geochemical analyses. However, harvesting of age class I scallops can sometimes be tricky as they are too small to be retained by scallop dredges or spotted by divers. Therefore, age class II+ scallops are often more easily captured. Our results did not reveal significant differences in the 2011 Mo : Ca time series in scallop shell portions formed between the 1st and 2nd winter growth check or after the 2nd winter growth check (Fig. 3), thus ruling out a possible ontogenetic effect on Mo and Li incorporation in shells. On the other hand, it seems that the springtime Li : Ca peak was more intense in shells of age class II scallops compared with younger specimens (average values: 233 and 161 μmol mol^{-1}, respectively; Fig. 3). However, a careful examination of these results suggests that this difference is mostly related to specimen N, which showed a much higher Li : Ca peak (392 μmol mol^{-1}) compared with other age class II specimens (194–201 μmol mol^{-1}). No satisfactory explanation can be put forward to elucidate this inter-individual variability. In any case, the spring environmental driver behind the incorporation of Mo and Li in calcitic shells of *P. maximus* very likely affected the entire population of scallops in the Bay of Brest, whatever their ontogenetic age or their living place was.

Spring bloom repercussions on shell geochemistry

The most striking features in age class I *P. maximus* shells are (1) the Mo : Ca peak recorded at the end of May 2011 and (2) the Li : Ca peak archived in mid-June 2011 (Fig. 4). As noticed in the previous section, these sudden increases in element levels likely occurred in all scallop shells from the Bay of Brest, whatever their age or sampling locality. This strongly suggests the existence of common environmental drivers responsible for the incorporation of large amounts of Mo and Li into the shells during the spring phytoplankton blooms (Fig. 9).

Mo : Ca ratio

Such a high inter-individual reproducibility has already been observed for Mo : Ca in scallop shells, including *P. maximus* (Barats et al. 2010) and *Decatopecten* (*Comptopallium*) *radula* (Thébault et al. 2009a). The incorporation of Mo in scallop shells could originate from both the dissolved and particulate phases in seawater. DMo usually appears to be conservative in the ocean (Collier 1985). Nevertheless, a systematic deficit in DMo was recorded over a 6-month period at the studied coastal station of Lanvéoc (January–June 2011), with a loss reaching 20 nmol L^{-1} (Fig. 8A). This was related to the incorporation of Mo in particles within the maximum turbidity zone of the inner estuary (Waeles et al. 2013). If phytoplankton activity was not responsible for DMo loss, this statement does not hold true for PMo. PMo concentrations were relatively low (< 0.1 nmol L^{-1}) over the period of January to March (Fig. 8A). Over this high freshwater discharge period (Aulne River water discharge ranging from 20 to 70 m^3 s^{-1}; Waeles et al. 2013), PMo should essentially correspond to lithogenic particles exported from the river/estuarine maximum turbidity zone. The beginning of PMo increase in April 2011 is clearly initiated with the onset of spring phytoplankton development. However, the uptake by phytoplankton cells, whose requirements have been estimated at 0.05–0.87 μmol of Mo mol^{-1} C (average = 0.22 μmol Mo mol^{-1} C; Ho et al. 2003), cannot alone explain the high increase of the PMo : POC ratio (from 5 to 15 μmol mol^{-1}) in April 2011 (Fig. 8B). Moreover, the increase of the PMo : POC ratio extended beyond the first spring bloom maximum, with values passing from 15 to 59 μmol mol^{-1} over the 2–19 May period. According to Dellwig et al. (2007), such an increase of PMo concentrations in coastal oxic waters, which is reinforced during the breakdown of an algae bloom, could be related to the formation of aggregates. These authors also indicate that Mo scavenging by organic matter and/or Mo reduction is promoted in the suboxic interior of aggregates and that leads to a sudden deposition of large amounts of organic matter enriched in Mo at the sediment–water interface.

This body of evidence strongly suggests a dietary origin of Mo incorporated in shells. The few studies which focused on Mo content in scallop soft tissues highlighted that, by far, the highest concentrations are found in the digestive gland where it could be one order of magnitude higher than in gills (Nørum et al. 2005; Tabouret et al. 2012). A similar distribution of Mo in soft parts was found in our study (Fig. 5A), giving additional strength to the following trophic pathway hypothesis. Indeed, the strongest uptake of metals bound to particulate material is achieved via the digestive gland, whereas gills and mantle are key interfaces for the uptake of dissolved metal ions from water (Marigómez et al. 2002).

The first spring phytoplankton bloom developed on winter nutrient stocks and reached its maximum intensity on 05 May 2011. However, phytoplankton was exposed to nutritional stress since the end of April 2011 because of silicate limitation. Such conditions favored exudation of extracellular polymeric substances by diatoms. This led to an increase of diatom stickiness and to the formation of diatom aggregates, which concentration likely reached its maximum in early May. The rapid sedimentation of these large particles immediately affected scallops, as evidenced by a significant shell growth rate reduction in the first week of May 2011 (Supporting Information Fig. S1). During their formation and transfer to the sediment, aggregates likely scavenged DMo, resulting in an increase of the PMo/POC ratio. Aggregate formation continued until the end of the bloom, resulting in a maximum PMo/POC ratio reached 2 weeks after the Chl *a* maximum. Although aggregates likely clogged scallop gills, thus hampering filtration and affecting shell growth negatively, it is highly probable that some Mo-enriched particles (the smallest ones) entered the digestive tract of the scallops. The maximum Mo concentration in soft tissues and in shells was reached

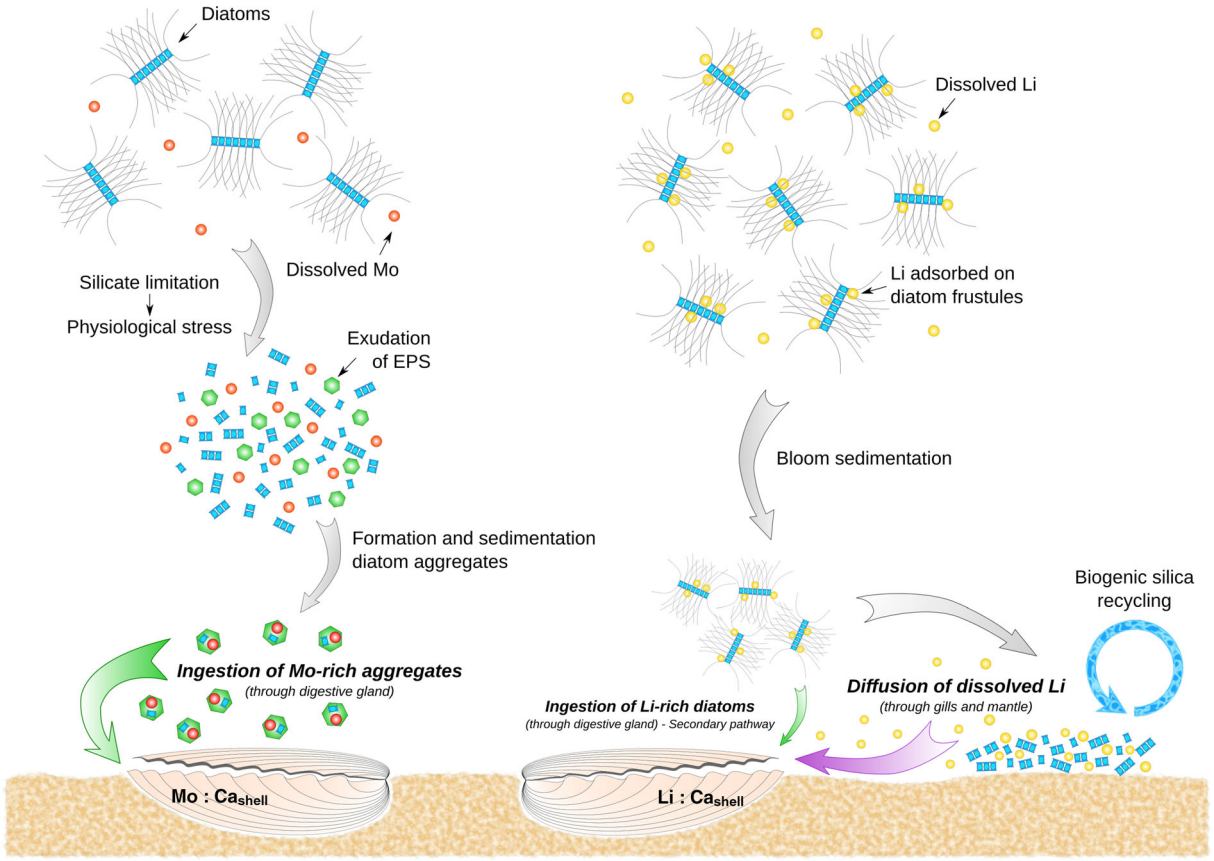

Fig. 9. Schematic illustration of the hypotheses for pathways of incorporation of Mo and Li in scallop shells.

simultaneously on 26–27 May 2011 (i.e., 1 week after the PMo/POC maximum), although it started to increase shortly after the first bloom maximum. This suggests that it took approx. 7–8 d between the entry of Mo in the digestive tract through particle filtration and its incorporation in scallop soft and hard tissues.

This line of reasoning tallies with one of the hypotheses put forward by Barats et al. (2010), who suggested that Mo : Ca maxima in *P. maximus* shells were directly influenced by spring changes of environmental conditions at the sediment–water interface, occurring shortly after an intense spring diatom bloom. They related the occurrence of these transient peaks with the extent of silicate depletion in the water column, which lead to the sedimentation of Mo-rich biogenic material at the sediment–water interface. Finally, our results confirm previous work by Tabouret et al. (2012) who worked in controlled experimental conditions with Mo isotope enrichments to explain the appearance of Mo:Ca peaks in *P. maximus* shells. Their study ruled out the assumption of Mo shell enrichment by the dissolved phase and concluded that these peaks likely had a dietary origin.

To conclude, our results suggest that the incorporation of Mo in scallop shells is related to the occurrence of diatom aggregate formation in the water column (Fig. 9). The timing of Mo : Ca peaks in shells could then be used as a proxy for the occurrence of Si limitation periods in coastal waters, while the height of these peaks likely reflects the amplitude of the first spring diatom bloom.

Li : Ca ratio

The overall pattern of the shell Li : Ca time series archived in the studied shells can be described as a relatively flat baseline around 40 μmol mol^{-1} interrupted with one main transient peak (average maximum value around 160 μmol mol^{-1}). Such a pattern is consistent with those retrieved in other studies dealing with bivalve shells, on *P. maximus* from the Bay of Brest (Thébault and Chauvaud 2013), on *Cerastoderma edula* from the North Sea (Füllenbach et al. 2015), or on *Megapitaria aurantiaca* from the Gulf of Panama (Sadatzki et al. 2019). On the other hand, bivalve shells from Arctic settings have a much lower baseline (around 10–15 μmol mol^{-1}) and do not display major Li:Ca peaks. This is the case for *Arctica islandica* in northern Iceland (Thébault et al. 2009*b*) and for *Serripes groenlandicus* and *Ciliatocardium ciliatum* in Svalbard (Vihtakari et al., 2017).

In the Bay of Brest, the main Li : Ca peak occurred on 18 June 2011 in shells and on 20 June 2011 in soft tissues (Figs. 4, 5). The time lag between these peaks and the first spring bloom is close to 7 weeks, while they occurred approx.

2 weeks after the second phytoplankton bloom. Thébault and Chauvaud (2013) already put forward the possible relationship between diatom blooms and Li incorporation in scallop shells. Indeed, it is known that biogenic opal production (e.g., originating from diatom frustules) is among the main removal processes of lithium from the ocean (Coplen et al., 2002). Therefore, we suggest that, in a way or another, incorporation of Li in scallops could be related to diatom blooms. Surprisingly, although the elemental composition of marine phytoplankton is well known, no information is available in the scientific literature on the lithium content in/on diatom cells. Here, we speculate that, like other minor elements, lithium is a component of diatom frustules. Whether lithium enters scallops through the dissolved phase or via a trophic pathway still needs to be investigated.

Contrary to molybdenum, lithium soft tissue concentrations were approx. twice as high in the mantle and the gills than in the digestive gland (Fig. 5B). All tissues presented an increase in Li content during the spring bloom period, suggesting that both dissolved Li (via gills and mantle) and particulate Li (via digestive gland) in the water column may be involved. During the first half of May 2011, Li concentration in the digestive gland ranged from 0.6 to 0.9 $\mu g\ g^{-1}$. These values are remarkably close to those found by Thibon et al. (2021) in digestive glands of *P. maximus* from the Bay of Biscay (0.8 $\mu g\ g^{-1}$). Then, a first increase in Li concentration (up to 1.8 $\mu g\ g^{-1}$) occurred on 26 May 2011, that is, 3 weeks after the first spring bloom. It was followed by a second maximum value approx. 2 weeks after the second spring bloom (2.4 $\mu g\ g^{-1}$ on 20 June 2011). As already noticed, these two blooms were almost exclusively composed of diatoms but differed in their Chl *a* content (approx. 1.5 times higher during the first bloom). In their study on juvenile *P. maximus* clearance rate, Strohmeier et al. (2009) highlighted that scallops have a nonlinear response to increasing food quantity, with the clearance rate decreasing as Chl *a* concentration increases (above a threshold around 0.4 $\mu g\ L^{-1}$). Therefore, our scallops could have assimilated similar amounts of food during these two spring blooms, explaining why the two peaks in Li concentrations in digestive glands were of comparable amplitude. The 2–3-week offset between diatom blooms and Li concentration maxima could be explained by the time required for a frustule to be dissolved in the digestive tract. If this trophic pathway was responsible alone for the incorporation of Li in shells, then two main Li : Ca peaks would have been encountered in the shells (instead of a single one; Fig. 4B). In addition, gills and mantle are the soft tissues with the highest Li concentration, strongly suggesting that Li also enters scallops through the dissolved pathway (Fig. 9).

At the end of a bloom, a significant amount of diatoms settles on the seafloor. Residence time of biogenic silica in sediments of the Bay of Brest is on the order of 1 month (Laruelle et al. 2009). The amount of Li exported to the sediment–water interface and then released during frustule dissolution likely depends (1) on the phytoplankton cell concentration during a bloom, and (2) on the surface available on diatom frustule for Li adsorption. Based on this estimate of the biovolume ratio between the first and second spring bloom, and considering that the frustule surface/volume ratio scales by a power of 2/3, it was calculated that the surface available on frustules for Li adsorption was approx. 2.6 times higher during the second bloom than during the first one. Interestingly, the Li concentration in gills and mantle measured 2–3 weeks after the second bloom was approx. 2.5 times higher than those measured 2–3 weeks after the first bloom. This strongly suggests that Li incorporated in gills and mantle originated from frustule dissolution at the sediment–water interface, a process that contributed to the increase in dissolved Li concentration in the neighborhood of scallops (Fig. 9).

In coastal ecosystems, diatoms are not only living in the water column but also on the sediment. These epibenthic diatoms are a major component of benthic microproducer communities, referred to as microphytobenthos. Their dynamics was investigated at Lanvéoc in 2011 and differed significantly from the phytoplankton dynamics (Chatterjee et al. 2013). Indeed, the microphytobenthic bloom was triggered by light and its biomass reached the annual maximum in mid-April 2011, as soon as maximum intensities of photosynthetically active radiations were recorded at the sediment–water interface. This 2-month time lag between the microphytobenthos bloom and the Li : Ca peak in scallop shells is greater than the residence time of biogenic silica in sediments (Laruelle et al. 2009). Therefore, although we cannot rule out a possible influence of epibenthic diatoms on the incorporation of Li in shells, it is quite clear that these microproducers cannot explain the mid-June Li : Ca_{shell} peak.

As Li : Ca spring time variations in shells more closely looked like changes in Li content in mantle and gills than in the digestive gland, it is concluded here that the incorporation of Li in scallop shells could be used as a proxy for the temporal dynamics (1) of diatom biovolume in the water column, and (2) of biogenic silica recycling at the sediment–water interface.

References

Alldredge, A., and C. Gotschalk. 1989. Direct observations of the mass flocculation of diatom blooms: Characteristics, settling velocities and formation of diatom aggregates. Deep-Sea Res. **36**: 159–171.

Barats, A., D. Amouroux, C. Pécheyran, L. Chauvaud, J. Thébault, and O. F. X. Donard. 2010. Spring molybdenum enrichment in scallop shells: A potential tracer of diatom productivity in temperate coastal environments (Brittany, NW France). Biogeosciences **7**: 233–245.

Berman, T., and D. A. Bronk. 2003. Dissolved organic nitrogen: A dynamic participant in aquatic ecosystems. Aquat. Microb. Ecol. **31**: 279–305.

Blondeau-Patissier, D., J. F. Gower, A. G. Dekker, S. R. Phinn, and V. E. Brando. 2014. A review of ocean color remote sensing methods and statistical techniques for the detection, mapping and analysis of phytoplankton blooms in coastal and open oceans. Prog. Oceanogr. **123**: 123–144.

Boyce, D., M. Lewis, and B. Worm. 2010. Global phytoplankton decline over the past century. Nature **466**: 591–596.

Chatterjee, A., and others. 2013. Comparative dynamics of pelagic and benthic micro-algae in a coastal ecosystem. Estuar. Coast. Shelf Sci. **133**: 67–77.

Cloern, J. E. 2001. Our evolving conceptual model of the coastal eutrophication problem. Mar. Ecol. Prog. Ser. **210**: 223–253.

Collier, R. W. 1985. Molybdenum in the Northeast Pacific Ocean. Limnol. Oceanogr. **30**: 1351–1354.

Coplen, T., and others. 2002. Isotope-abundance variations of selected elements (IUPAC technical report). Pure Appl. Chem. **74**: 1987–2017.

Crocker, K. M., and U. Passow. 1995. Differential aggregation of diatoms. Mar. Ecol. Prog. Ser. **117**: 249–257.

Del Amo, Y., O. Le Pape, P. Tréguer, B. Quéguiner, A. Ménesguen, and A. Aminot. 1997. Impacts of high-nitrate freshwater inputs on macrotidal ecosystems. I. Seasonal evolution of nutrient limitation for the diatom-dominated phytoplankton of the Bay of Brest (France). Mar. Ecol. Prog. Ser. **161**: 213–224.

Dellwig, O., M. Beck, A. Lemke, M. Lunau, K. Kolditz, B. Schnetger, and H.-J. Brumsack. 2007. Non-conservative behaviour of molybdenum in coastal waters: Coupling geochemical, biological, and sedimentological processes. Geochim. Cosmochim. Acta **71**: 2745–2761.

Doré, J., G. Chaillou, P. Poitevin, P. Lazure, A. Poirier, L. Chauvaud, P. Archambault, and J. Thébault. 2020. Assessment of Ba/Ca in *Arctica islandica* shells as a proxy for phytoplankton dynamics in the Northwestern Atlantic Ocean. Estuar. Coast. Shelf Sci. **237**: 106628.

Field, C. B., M. J. Behrenfeld, J. T. Randerson, and P. G. Falkowski. 1998. Primary production of the biosphere: Integrating terrestrial and oceanic components. Science **281**: 237–240.

Füllenbach, C. S., B. R. Schöne, and R. Mertz-Kraus. 2015. Strontium/lithium ratio in aragonitic shells of *Cerastoderma edule* (Bivalvia)—A new potential temperature proxy for brackish environments. Chem. Geol. **417**: 341–355.

Gillikin, D. P., A. Lorrain, Y.-M. Paulet, L. André, and F. Dehairs. 2008. Synchronous barium peaks in high-resolution profiles of calcite and aragonite marine bivalve shells. Geo-Mar. Lett. **28**: 351–358.

Hickel, W. 1998. Temporal variability of micro- and nanoplankton in the German Bight in relation to hydrographic structure and nutrient changes. ICES J. Mar. Sci. **55**: 600–609.

Ho, T.-Y., A. Quigg, Z. V. Finkel, A. J. Milligan, K. Wyman, P. G. Falkowski, and F. M. M. Morel. 2003. The elemental composition of some marine phytoplankton. J. Phycol. **39**: 1145–1159.

Laruelle, G., and others. 2009. Benthic-pelagic coupling and the seasonal silica cycle in the Bay of Brest (France): New insights from a coupled physical-biological model. Mar. Ecol. Prog. Ser. **385**: 15–32.

Lorrain, A., Y.-M. Paulet, L. Chauvaud, N. Savoye, E. Nezan, and L. Guérin. 2000. Growth anomalies in *Pecten maximus* from coastal waters (Bay of Brest, France): Relationship with diatom blooms. J. Mar. Biol. Assoc. UK **80**: 667–673.

Mackas, D. 2011. Does blending of chlorophyll data bias temporal trend? Nature **472**: E4–E5.

Marchais, V., and others. 2015. Coupling experimental and field-based approaches to decipher carbon sources in the shell of the great scallop, *Pecten maximus* (L.). Geochim. Cosmochim. Acta **168**: 58–69.

Marigómez, I., M. Soto, M. P. Cajaraville, E. Angulo, and L. Giamberini. 2002. Cellular and subcellular distribution of metals in molluscs. Microsc. Res. Tech. **56**: 358–392.

Mook, W., and J. Vogel. 1968. Isotopic equilibrium between shells and their environment. Science **159**: 874–875.

Moschonas, G., R. J. Gowen, R. F. Paterson, E. Mitchell, B. M. Stewart, S. McNeill, P. M. Glibert, and K. Davidson. 2017. Nitrogen dynamics and phytoplankton community structure: The role of organic nutrients. Biogeochemistry **134**: 125–145.

Nørum, U., V. W. M. Lai, and W. R. Cullen. 2005. Trace element distribution during the reproductive cycle of female and male spiny and Pacific scallops, with implications for biomonitoring. Mar. Pollut. Bull. **50**: 175–184.

Olenina, I., and others. 2006. Biovolumes and size-classes of phytoplankton in the Baltic Sea. HELCOM Baltic Sea Environ. Proc. **106**: 1–144.

Passow, U. 2000. Formation of transparent exopolymer particles, TEP, from dissolved precursor material. Mar. Ecol. Prog. Ser. **192**: 1–11.

Peharda, M., B. Schöne, B. Black, and T. Corrège. 2021. Advances of sclerochronology research in the last decade. Palaeogeogr., Palaeoclimatol. Palaeoecol. **570**: 110371.

Poulain, C., D. P. Gillikin, J. Thébault, J.-M. Munaron, M. Bohn, R. Robert, Y.-M. Paulet, and A. Lorrain. 2015. An evaluation of Mg/Ca, Sr/Ca, and Ba/Ca ratios as environmental proxies in aragonite bivalve shells. Chem. Geol. **396**: 42–50.

Quéguiner, B., and P. Tréguer. 1984. Studies on the phytoplankton in the Bay of Brest (Western Europe). Seasonal variations in composition, biomass and production in relation to hydrological and chemical features (1981–1982). Bot. Mar. **27**: 449–459.

R Core Team (2020) R: A language and environment for statistical computing. R Foundation for Statistical Computing, Vienna, Austria. Available from https://www.R-project.org/.

Ragueneau, O., E. De Blas Varela, P. Tréguer, B. Quéguiner, and Y. Del Amo. 1994. Phytoplankton dynamics in relation

to the biogeochemical cycle of silicon in a coastal ecosystem of Western Europe. Mar. Ecol. Prog. Ser. **106**: 157–172.

Rousseaux, C. S., and W. W. Gregg. 2014. Interannual variation in phytoplankton primary production at a global scale. Remote Sens. (Basel) **6**: 1–19.

Sadatzki, H., M. Alberti, D. Garbe-Schönberg, N. Andersen, P. Strey, H. Fortunato, C. Andersson, and P. Schäfer. 2019. Paired Li/Ca and $\delta^{18}O$ peaks in bivalve shells from the Gulf of Panama mark seasonal coastal upwelling. Chem. Geol. **529**: 119295.

Strohmeier, T., Ø. Strand, and P. Cranford. 2009. Clearance rates of the great scallop (*Pecten maximus*) and blue mussel (*Mytilus edulis*) at low natural seston concentrations. Mar. Biol. **156**: 1781–1795.

Tabouret, H., S. Pomerleau, A. Jolivet, C. Pécheyran, R. Riso, J. Thébault, L. Chauvaud, and D. Amouroux. 2012. Specific pathways for the incorporation of dissolved barium and molybdenum into the bivalve shell: An isotopic tracer approach in the juvenile great scallop (*Pecten maximus*). Mar. Environ. Res. **78**: 15–25.

Thébault, J., L. Chauvaud, S. L'Helguen, J. Clavier, A. Barats, S. Jacquet, C. Pécheyran, and D. Amouroux. 2009*a*. Barium and molybdenum records in bivalve shells: Geochemical proxies for phytoplankton dynamics in coastal environments? Limnol. Oceanogr. **54**: 1002–1014.

Thébault, J., B. R. Schöne, N. Hallmann, M. Barth, and E. V. Nunn. 2009*b*. Investigation of Li/Ca variations in aragonitic shells of the ocean quahog *Arctica islandica*, Northeast Iceland. Geochem. Geophys. Geosyst. **10**: Q12008.

Thébault, J., and L. Chauvaud. 2013. Li/Ca enrichments in great scallop shells (*Pecten maximus*) and their relationship with phytoplankton blooms. Palaeogeogr. Palaeoclimatol. Palaeoecol. **373**: 108–122.

Thibon, F., L. Weppe, N. Vigier, C. Churlaud, T. Lacoue-Labarthe, M. Metian, Y. Cherel, and P. Bustamante. 2021. Large-scale survey of lithium concentrations in marine organisms. Sci. Total Environ. **751**: 141453.

Thornton, D. C. O. 2002. Diatom aggregation in the sea: Mechanisms and ecological implications. Eur. J. Phycol. **37**: 149–161.

Vihtakari, M., and others. 2017. A key to the past? Element ratios as environmental proxies in two Arctic bivalves. Palaeogeogr. Palaeoclimatol. Palaeoecol. **465**: 316–332.

Waeles, M., G. Dulaquais, A. Jolivet, J. Thébault, and R. Riso. 2013. Systematic non-conservative behavior of molybdenum in a macrotidal estuarine system (Aulne-Bay of Brest, France). Estuar. Coast. Shelf Sci. **131**: 310–318.

Warner, A., and G. Hays. 1994. Sampling by the continuous plankton recorder survey. Prog. Oceanogr. **34**: 237–256.

Acknowledgments

We kindly acknowledge Beatriz Beker (Centre d'Océanologie de Marseille/Institut Universitaire Européen de la Mer, France) for counting and identification of phytoplankton species, and Claire Bassoullet (Laboratoire Domaines Océaniques, Université de Bretagne Occidentale, France) and Gaëlle Barbotin (IPREM, Pau, France) for elemental analyses of scallop shells. We are also grateful to the SOMLIT-Brest (Service d'Observation en Milieu LITtoral, INSU-CNRS) and PACHIDERM (Plateau d'Analyse CHImique de l'EnviRonnement Marin) groups responsible for water sampling, analysis, and data management. Special thanks to Franck Quéré and Daniel Morigeon (R/V Albert Lucas) for their priceless help during the cruises (as well as for the friendly aperos). This manuscript benefited from critical reviews and very helpful comments by K. David Hambright (Editor-in-Chief), Christelle Not (Associate Editor), and two anonymous reviewers. This work was supported by the CHIVAS (ANR-09-BLAN-0335-01) and HIPPO (ANR-18-CE92-0036-01) projects, both funded by the French National Research Agency.

Submitted 02 July 2021
Revised 18 October 2021
Accepted 31 October 2021

Associate editor: Christelle Not